OPEN ACCESS
IOP Publishing
Journal of Optics
J. Opt. **27** (2025) 025103 (9pp)
https://doi.org/10.1088/2040-8986/ada6d5

Topology of Bloch impedance: traveling waves, dispersive media, and electromagnetic energy

Igor Tsukerman[1,*] **and Vadim A Markel**[2]

[1] Department of Electrical and Computer Engineering, The University of Akron, Akron, OH 44325-3904, United States of America
[2] Departments of Radiology, University of Pennsylvania, Philadelphia, PA 19104, United States of America

E-mail: igor@uakron.edu

Received 19 July 2024, revised 8 October 2024
Accepted for publication 7 January 2025
Published 28 January 2025

Abstract

The bulk-boundary correspondence (b-bc) principle, which relates interface modes between two periodic structures to topological invariants of the respective Bloch bands, is widely accepted in electrodynamics. However, this acceptance stems largely from condensed matter (CM) theories. It is desirable to establish direct connections between the topological principles and Maxwell electrodynamics, rather than relying on CM results. Such connections have in recent years been found in the case of standing evanescent waves in periodic dielectric media. This paper extends these analyses to waves propagating along an interface between two periodic structures, possibly with frequency-dependent dielectric permittivities. The paper shows that the b-bc principle continues to hold for any physically realizable structures, in which the density of electromagnetic energy must be positive. The paper rigorously proves that in this physically valid case impedance of traveling interface modes within any given bandgap decreases monotonically as a function of frequency.

Keywords: photonic band gap materials, heterostructures, optical properties, topological photonics

1. Introduction

Topological concepts in condensed matter (CM) physics have been developed and extensively studied since the discovery of the quantum Hall effect in the 1980s (see reviews [1, 2] and references there). Central in these studies is the bulk-boundary correspondence (b-bc) principle, which relates the existence and number of boundary modes at interfaces of periodic structures to the topological invariants of the respective Bloch bands [3, 4].

In 2008–2009, the CM results started to be translated to electrodynamics and photonics [5–7]. This translation has a high empirical value and has made a significant impact in applications. However, along with the similarities, there are obvious principal differences between CM phenomena and electrodynamics. From the perspective of theoretical physics, the fundamental distinction is between electrons as fermions and photons as bosons. Electrons carry electric charge and, in contrast with photons, interact with magnetic fields, which is critical in the vast majority of applications. The physical and mathematical models of the two classes of problems are quite different.

A case in point is the ingenious analysis [8, 9] of the topological features of Harper's equation—a special one-dimensional three-point difference scheme relevant to the

* Author to whom any correspondence should be addressed.

quantum Hall effect but having only a tenuous connection with problems of photonics. Another important case is lattice models corresponding to tight-binding bulk Hamiltonians; sophisticated mathematical tools of algebraic topology (K-theory) have been brought to bear on such problems [4, 10, 11]. While the utility of lattice models in solid state physics is indisputable ([10], [4, p 23]), their relevance to electrodynamics is, at best, debatable. Yet another example is the coupled resonator model of [12, pp 12–18], which is valuable but constitutes a phenomenological approximation.

With the above in mind, it is desirable to establish direct connections between topological principles and partial differential equations of Maxwell electrodynamics, rather than inferring those connections in a roundabout way from various lattice models and CM theories. Steps in that direction have already been taken. The starting point was [13], where the importance of electromagnetic boundary impedance for the b-bc principle was emphasized. Moreover, this principle was proved in [13] by direct algebraic calculation for periodic layered media with mirror-symmetric lattice cells, two different dielectric materials per cell, and evanescent *standing* waves. This was a major advance, but the direct algebra for two layers is not generalizable to arbitrary periodic media.

Such generalizations were recently put forward by several research groups [14–17], but restrictions still remain. These published analyses apply only to *non-propagating* waves. Frequency dispersion of the dielectric function was considered in [16]. In [17], a principal new feature is the analysis of Bloch impedance as a function of two *complex-valued* parameters: frequency and the Bloch eigenvalue. Impedance and the Bloch wavenumber q are formally introduced below, but in the present paper, the frequency is still assumed real. Our previous analysis [15] and relevant proofs are extended to periodic media with frequency-dependent permittivity and waves propagating along the interface. Both extensions are of great mathematical and physical interest. Especially critical for applications are robust topologically protected unidirectional interface modes, which cannot be accounted for in the analyses of standing waves.

While these generalizations are substantial, several restrictive assumptions are still made. The lattice cells are assumed in the present paper to have mirror symmetry, which is an essential feature of topological models, as emphasized in a variety of publications [13, 14, 18–20]. The physical reason for this assumption is that the presence or absence of interface modes is intimately connected with the symmetry (parity) of Bloch modes at the band edges. These modes have a definite parity (i.e. are either symmetric or antisymmetric) only if the cells are themselves symmetric; this stems from the fact that the differential operator of the problem commutes with the symmetry operator. Zak phase has discrete values 0 or π only for symmetric cells [3, 18]; otherwise this phase can take on any value. Consequently, the b-bc principle cannot, strictly speaking, even be formulated—let alone proved—for non-symmetric cells. Nevertheless our numerical results show that the interface modes survive under small asymmetric perturbations of the cells, which is not entirely surprising due to continuity.

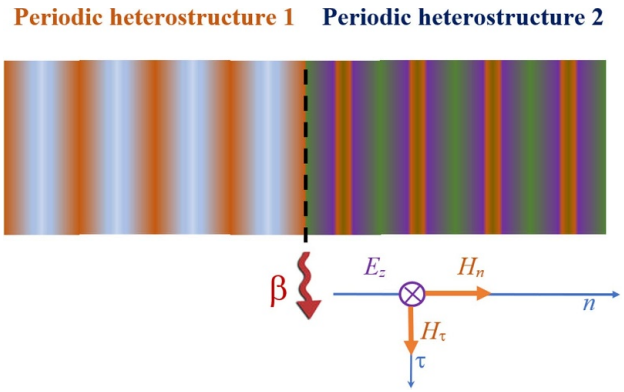

Figure 1. Setup for a boundary wave propagating along an interface between two heterostructures (1D photonic crystals). The *s*-mode is considered, with the electric field perpendicular to the plane of the picture and the magnetic field in the plane. The interface is at $n = 0$ (dashed line). A possible mode may propagate along the boundary with a (real) phase constant β, while evanescently decaying in both directions away from the interface.

In this paper, losses are assumed negligible, which leaves non-Hermitian topological photonics [21, 22] outside the scope of this paper. Other topological issues, such as waveguides [23, 24] and valley photonics (including the 'photonic spin Hall effect' on hexagonal lattices [20, 25]), are not covered either. However, the concepts and methods discussed here can be applied to these problems.

2. Formulation of the electromagnetic problem

We consider two structures, each of which is periodic in its respective half space (figure 1) and introduce a right-handed Cartesian system (n, τ, z) to study waves in one of these structures. Clearly, analysis pertaining to the other one is completely analogous, but interface matching conditions play a critical role in the end. The n and τ directions are normal and tangential to the interface, respectively, while the z axis is perpendicular to the plane of the picture. All material parameters are assumed to depend only on n; this setup includes, but is not limited to, the case of layered media. Subscripts 1 and 2 will indicate the structures on the left and right sides of the interface, respectively. For uniformity of mathematical expressions and without much risk of confusion, these subscripts will not be used for the n coordinate which, for each of the structures, is assumed to be directed *away* from the interface.

A linear electromagnetic problem at a given frequency ω is considered. For brevity, we assume throughout the paper intrinsically nonmagnetic materials:

$$\mu(n) = 1 \tag{1}$$

Extending our analysis to simple magnetic media is straightforward, by full analogy with [15]; the case of gyromagnetic media is algebraically more complicated and relegated to future research.

The dielectric permittivity $\epsilon(n,\omega)$ can be frequency dependent; but, as noted above, losses, and hence the imaginary part of ϵ, are neglected. Due to the assumed mirror symmetry of the lattice cells,

$$\epsilon(a-n,\omega) \;=\; \epsilon(n,\omega) \tag{2}$$

These properties hold for all n, $a-n$ within a given medium; a is its lattice period in the n direction. Dependence of physical quantities on the frequency ω may not always be explicitly indicated. We assume the s-mode (one-component electric field $\mathbf{E}=\hat{\mathbf{z}}E$); analysis for the p-mode is similar. In the tangential direction, the fields are assumed to vary as [26]

$$\begin{aligned} E(n,\tau,s) &= e(n,s)\exp(i\beta\tau)\\ \mathbf{H}(n,\tau,s) &= \mathbf{h}(n,s)\exp(i\beta\tau)\\ \mathbf{h}(n,s) \;&=\; h_n(n,s)\,\hat{\mathbf{n}} + h_\tau(n,s)\,\hat{\boldsymbol{\tau}},\\ s &= k^2 \end{aligned} \tag{3}$$

Unit vectors are marked with hats; $k=\omega/c$ is the wave number; $-\infty<\beta<\infty$ is a given parameter. Note that in the τ direction the medium is assumed homogeneous; hence there are no Brillouin zones unless an artificial τ-periodicity is introduced for one reason or another. Naturally, $e(n,s)$ is defined up to a factor and can be made unique by any suitable normalization.

The complex amplitudes $\mathbf{E}=\mathbf{E}(n,\tau,s)$ and $\mathbf{H}=\mathbf{H}(n,\tau,s)$ satisfy Maxwell's equations; for nonmagnetic media,

$$\nabla\times\mathbf{E} = ik\mathbf{H}, \quad \nabla\times\mathbf{H} = -ik\epsilon\mathbf{E} \tag{4}$$

in the Gaussian system; the phasor convention is $\exp(-i\omega t)$.

We refer to the problem under consideration symbolically as '1.5D' because the magnetic field and wave vector have two physical components, while mathematically (4) can be reduced to a 1D equation for the s-mode:

$$e''(n,s) \;+\; s\epsilon(n,s)\,e(n,s) - \beta^2 e(n,s) \;=\; 0 \tag{5}$$

Primes always indicate the n-derivatives; s-derivatives will be indicated explicitly as ∂_s.

Evanescent modes, by definition, decay at infinity:

$$\lim_{n\to\infty} e(n,s) = 0; \quad \lim_{n\to\infty}\mathbf{h}(n,s) = 0 \tag{6}$$

The Maxwell interface condition between the structures can be defined via electromagnetic impedance Z or, equivalently, via the 'mathematical impedance' $\xi(s)$ [13–16, 23]:

$$Z_1(0,s)+Z_2(0,s) \;=\; 0 \quad\Leftrightarrow\quad \xi_1(0,s)+\xi_2(0,s) \;=\; 0, \tag{7}$$

the impedances being defined as follows:

$$Z(n,s) \overset{\text{def}}{=} \frac{e(n,s)}{h_\tau(n,s)} \tag{8}$$

$$\xi(n,s) \overset{\text{def}}{=} \frac{e(n,s)}{e'(n,s)} = \frac{Z(n,s)}{ik} \tag{9}$$

Especially important are the boundary values $Z(0,s)=Z(a,s)$, $\xi(0,s)=\xi(a,s)$. If $h_\tau(0,s)=0$ or, alternatively, $e(0,s)=0$, we say that impedance has a pole or a null, respectively. Poles and nulls of impedance at the Γ and X points are of particular interest.

Clearly, the 1.5D setup is different from that of a 2D electromagnetic crystal with inclusions in lattice cells; however, since topological effects are robust, the 1.5D case does provide important insights, while being amenable to analytical treatment.

Let us recall the key ingredients of the existing b-bc proofs [14–16] and see how these proofs can be generalized to the 1.5D problem.

First, for pure dielectrics, it has already been shown that impedance at the Γ and X points (i.e. $\mathrm{Re}\,q=0,\pm\pi a$, where q is the Bloch number in the n direction) within any gap is real and changes monotonically either from $+\infty$ to zero or, alternatively, from zero to $-\infty$, as frequency increases from the bottom to the top of the gap [14–16]. In the first case, when Z or ξ start with a pole, we say that the gap is of type p; in the second case, the gap is said to be of type n [15]. The poles and nulls of impedance correspond to symmetric and antisymmetric modes, respectively, where symmetry is defined with respect to the electric field. The boundary condition (7) is satisfied at a certain frequency if and only if the gaps are of opposite type for the two structures—i.e. for a 'pn' junction [15].

Second, if one traces the zeros and poles of Z or ξ from a particular frequency in a given gap all the way down to the zero frequency, it becomes clear that the type of that gap depends on how many changes from a pole to a zero and back the impedance undergoes in this process. For dielectric structures, impedance always changes from a pole to a zero or from a zero to a pole across any gap; this can be deduced from the oscillation theorem for the Sturm–Liouville problem [16, 27]. Whether or not similar changes occur across a given *band* depends on the Zak phase [11, 14–16, 18] of that band.

Strictly speaking, critical for the proof is the continuous change of Z or ξ between a pole and a null in the gap, and not the monotonicity of that change. However, the latter is a physically meaningful property guaranteeing uniqueness of an interface mode in addition to its existence.

In passing, let us note that there exists a treatment of the problem via 'effective mass,' defined in [28] in terms of the effective permittivity and permeability ϵ_{eff} and μ_{eff}. Namely, $\epsilon_{\text{eff}}=|n_{\text{eff}}|/(k\xi_{\text{eff}}$, and $\mu_{\text{eff}}=-|n_{\text{eff}}|\,k\xi_{\text{eff}}$, where n_{eff} is the effective index. Hence the sign of impedance ξ is in a one-to-one correspondence with the signs of the permittivity and permeability. Our preference is to deal with impedance as a manifestation of Maxwell's boundary conditions rather than with effective parameters which require a nontrivial homogenization procedure in addition.

3. Monotonicity of impedance in bandgaps

We wish to generalize the proofs of [14–16] to traveling waves (β not necessarily zero), taking the frequency dependence of

ϵ into account. To examine the monotonicity of $\xi(s)$, one differentiates (9):

$$\partial_s \xi(s) = \frac{g(0,s)\, e'(0,s) - e(0,s)\, g'(0,s)}{e'(0,s)^2} \tag{10}$$

Since all parameters in the governing equation (5) are assumed real, and so are the evanescent boundary conditions (6) in the n direction and periodic conditions for e, $\mathbf{h}$ in the τ direction, $e(n,s)$ can also be taken as real. Differentiating the governing equation (5) with respect to s, we have

$$g''(n,s) + w(n,s)\, e(n,s) + s\epsilon(n,s)\, g(n,s) - \beta^2 g(n,s) = 0 \tag{11}$$

$$g(n,s) = \partial_s e(n,s), \quad w(n,s) = \partial_s(s\epsilon(n,s)) \tag{12}$$

As a mathematically minor but physically important deviation from the previous analyses [14–16], here we have kept the term $s\epsilon$ together rather than differentiating the factors separately. The physical meaning of that becomes evident toward the end of our derivation.

We multiply (11) by $e(n,s)$ (which is real) and combine the terms containing $g(n,s)$:

$$g''(n,s)\, e(n,s) + \left[s\epsilon(n,s)\, e(n,s) - \beta^2 e(n,s)\right] g(n,s) + w(n,s)\, e^2(n,s) = 0 \tag{13}$$

The expression in the square brackets simplifies due to (5):

$$g''(n,s)\, e(n,s) - e''(n,s)\, g(n,s) + w(n,s)\, e^2(n,s) = 0 \tag{14}$$

Integrating this equation over $\Omega = [0,\infty)$ and applying Green's identity to the first two terms, one obtains

$$g(0,s)\, e'(0,s) - e(0,s)\, g'(0,s) + \int_0^\infty w(n,s)\, e^2(n,s)\, \mathrm{d}n = 0 \tag{15}$$

The signs of the boundary terms ($n=0$) reflect the fact that n is directed *into* the domain Ω. Comparing this equation with (10), we finally have

$$\partial_s \xi(s)\, e'(0,s)^2 = -\int_0^\infty w(n,s)\, e^2(n,s)\, \mathrm{d}n \tag{16}$$

It follows that

$$\text{If } w(n,s) = \partial_s(s\epsilon(n,s)) > 0 \text{ then } \partial_s \xi(s) < 0 \tag{17}$$

within any gap away from the poles of impedance.

Let us recall that the energy density in a dispersive dielectric medium is proportional to the Brillouin-Landau–Lifshitz term $w_{\mathrm{BLL}} = \partial_\omega(\omega\,\epsilon(\omega))$ [29, p 92], [30, section 80, section 84]. It is instructive to compare this expression with the definition of $w(n,s)$:

$$w_{\mathrm{BLL}} = \partial_\omega(\omega\,\epsilon(n,\omega)) = \epsilon(n,\omega) + \omega\,\partial_\omega \epsilon(n,\omega) \tag{18}$$

$$w(n,\omega) = \partial_s(s\epsilon(n,s)) \overset{s=\omega^2/c^2}{=} \epsilon(n,\omega) + \frac{1}{2}\omega\,\partial_\omega \epsilon(n,\omega) \tag{19}$$

In (18), we inserted the dependence on n for the sake of uniformity of all expressions involving the dielectric permittivity. One may now note a hierarchy of conditions on frequency dispersion for which the b-bc holds:

1. [Strongest.] $\partial_\omega \epsilon(n,\omega) > 0$.
2. [Less restrictive.] $w_{\mathrm{BLL}} = \epsilon(n,\omega) + \omega\,\partial_\omega \epsilon(n,\omega) > 0$.
3. [Least restrictive.] $w = \epsilon(n,\omega) + \frac{1}{2}\omega\,\partial_\omega \epsilon(n,\omega) > 0$.

For brevity, the real part of ϵ is implied in all three conditions. According to the derivation in [30], Condition 1 (the strongest) in the transparency window of any physically realizable materials follows from the Kramers–Kronig relations. However, this derivation depends on the behavior of $\mathrm{Im}\,\epsilon(n,\omega')/(\omega'^2-\omega^2)$ in the vicinity of a given frequency ω. If $\mathrm{Im}\,\epsilon(n,\omega')$ is *exactly* zero for $\omega' \approx \omega$, then Condition 1 follows strictly; but if the material is *almost* transparent ($\mathrm{Im}\,\epsilon(n,\omega')$ is small but nonzero), all bets are off.

Condition 2 – the positivity of electromagnetic energy density—must hold for all physical systems. Condition 3, which has emerged in our study, is slightly less restrictive with respect to $\partial_\omega \varepsilon$ due to the extra factor of 1/2, while the analysis of [16] involves Condition 1. Apart from these distinctions, a physically important observation is that, at least in the 1.5D setup, *the b-bc principle is closely linked to the positivity of electromagnetic energy density*.

The numerical examples below illustrate this conclusion and also demonstrate that the opposite statement is true, too. Namely, if the positivity of energy is violated (in a hypothetical medium), then the b-bc principle may not hold either.

4. Numerical Illustration

As an example, we consider layered media with mirror-symmetric lattice cells containing three layers of widths $a/4$, $a/2$, $a/4$. The first and third layer are air; parameters of the second layer may vary. In contrast with our previous publications [15, 31, 32], where similar examples were presented, the middle layer may have frequency-dependent dielectric properties.

To illustrate the results of the previous section, we compare two cases of frequency dispersion—normal (physically realizable—figure 2, equation (20)) and anomalous (figure 3, equation (21)). In the figures and expressions, the normalized frequency is $f = a/\lambda$.

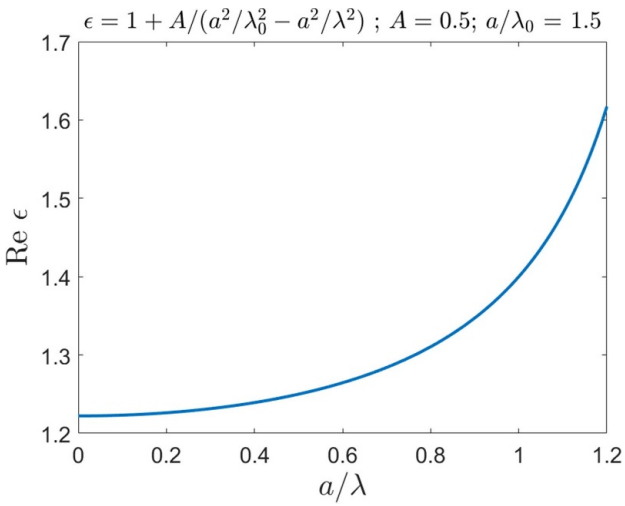

Figure 2. Frequency dependence of ϵ for the example Drude model (parameters are indicated in the text). The frequency axis is scaled as a/λ for consistency through all plots.

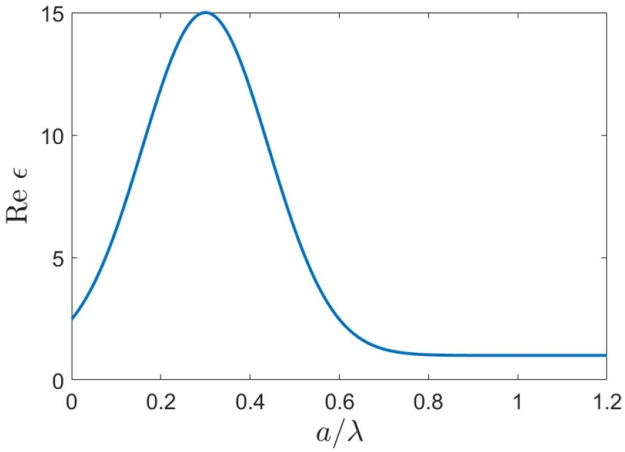

Figure 3. An artificial ϵ with anomalous dispersion; parameters are indicated in the text.

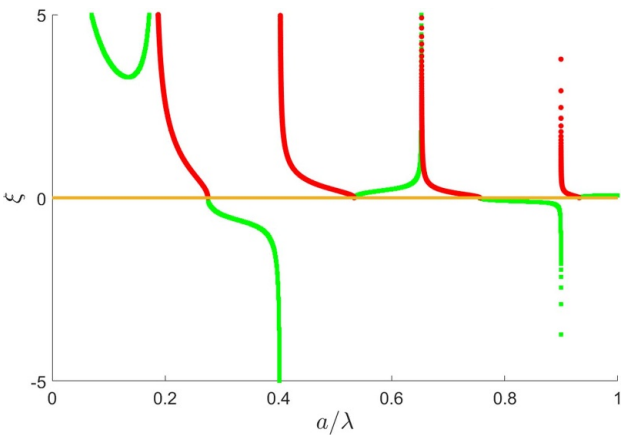

Figure 4. Mathematical impedance $\xi(0)$ as a function of a/λ for the Drude-model example; parameters are indicated in the text. The red curves correspond to Re ξ in the gaps, and the green curves—to Im ξ in the bands. These plots are for $\beta = 0$. Note that (i) ξ, unlike Z, has a pole at the zero frequency; (ii) Re ξ corresponds to Im Z, and vice versa; see (9).

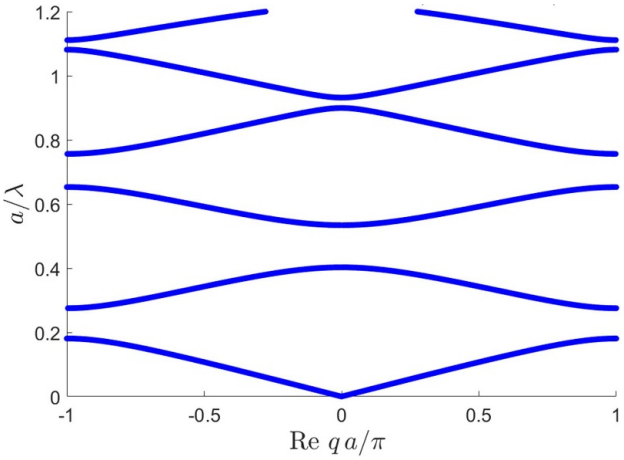

Figure 5. Bloch bands for the Drude-model example; parameters are indicated in the text.

$$\epsilon = 1 + \frac{A}{f_0^2 - f^2} \tag{20}$$

and

$$\epsilon = 1 + C\exp\left(-\frac{(f-f_0)^2}{\alpha^2}\right)$$
$$C = 14;\ \ f_0 = 0.3;\ \ \alpha = 0.2 \tag{21}$$

In the case of normal dispersion, our analysis has shown that impedance must be monotonically decreasing in the gaps. This result is numerically illustrated in figure 4. The red curves in that figure correspond to the real part of ξ in the gaps, and the green curves—to the imaginary part of ξ in the bands. The respective band diagram is displayed in figure 5 for reference.

With these preliminaries in place, we can now present some illustrative cases of boundary modes. In our first example, the middle layers of the two abutting heterostructures—with simple and Drude media, respectively—have the following properties. For the simple structure (left of the interface): $\epsilon = 20$, $\mu = 3$. For the Drude structure (right of the interface): $A = 0.5, \mu = 3, f_0 = 2$ (20). For the phase parameter $\beta a = \pi/6$, the mode has been calculated to exist—i.e. impedance matching holds—at the normalized frequency $a/\lambda \approx 0.6877$. Since $ka = 2\pi\, a/\lambda \approx 4.32 \gg \beta a = \pi/6$, this mode can be excited by external illumination similarly to the modes in [13, 28].That is in contrast with surface plasmon polariton-like modes, which, due to the large tangential wavenumber, require special excitation configurations [33–35]. The interface mode as a function of n is plotted in figure 6, and its time evolution is illustrated by a series of snapshots in figure 7.

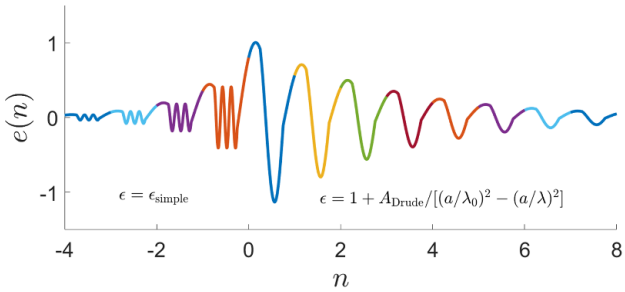

Figure 6. The electric field of an interface mode as a function of the normal coordinate n. Each cell of each structure has three layers with widths $0.25a, 0.5a, 0.25a$; the first and third layer have $\epsilon = 1$, $\mu = 1$. The middle layers have the following properties. For the simple structure (left of the interface): $\epsilon = 20$, $\mu = 3$. For the Drude structure (right of the interface): $A = 0.5$, $\mu = 3, f_0 = 2$. The mode propagates at the normalized frequency $a/\lambda \approx 0.6877$; $\beta a = \pi/6$.

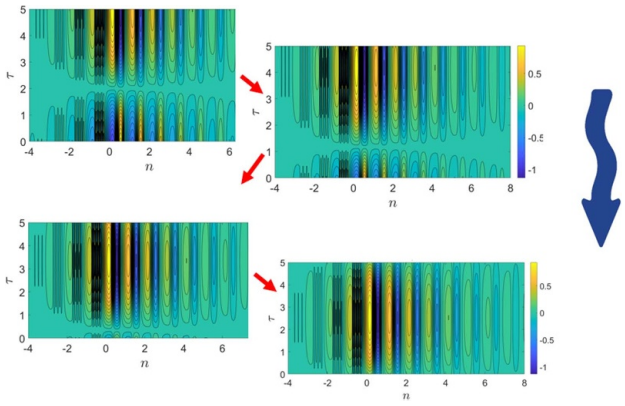

Figure 7. Time evolution snapshots of the mode shown in figure 6, at the moments of time $t = 0, 0.1, 0.2, 0.3$. The time sequence is indicated with the red arrows, and the direction of propagation of the wave — with a thick curvy arrow on the right.

To gauge the robustness of this mode, we consider its behavior under small perturbations of parameters. An interesting question is whether the mode survives if the mirror symmetry of the lattice cell gets broken. Suppose the width of the middle layer is reduced by 10%, from $0.5a$ to $0.45a$, with the corresponding increase of the width of the third layer from $0.25a$ to $0.3a$, so that the cell size is still normalized to unity. Notably, even though the theory applies only to mirror-symmetric cells, the mode persists (figure 8), with the normalized frequency shifting to $a/\lambda \approx 0.73655$.

As a different minor perturbation, consider increasing the permittivity of the middle layer in the simple medium by 5% from $\epsilon = 20$ to $\epsilon = 21$. The mode still exists at the normalized frequency $a/\lambda \approx 0.6808$, all other parameters remaining unchanged (figure 9).

For *anomalous dispersion*, impedance may not be a monotonic function of frequency. This is demonstrated by Figure 10, with the respective Bloch bands shown in figure 11 for reference. It may come as a surprise that one of the bands, around $a/\lambda \sim a/\lambda_0 = 0.3$ does not extend to the band edges

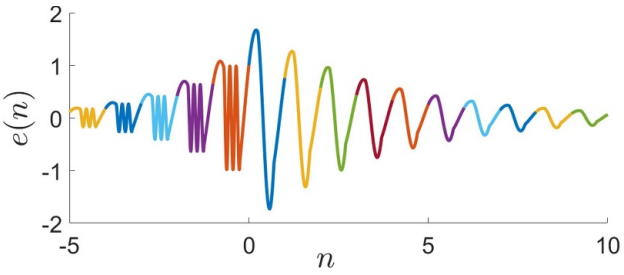

Figure 8. Same as figure 6, but the width of the middle layer in the lattice cell is reduced 10% from $0.5a$ to $0.45a$, with the commensurate increase in the width of the third layer. The mode persists at the normalized frequency $a/\lambda \approx 0.73655$.

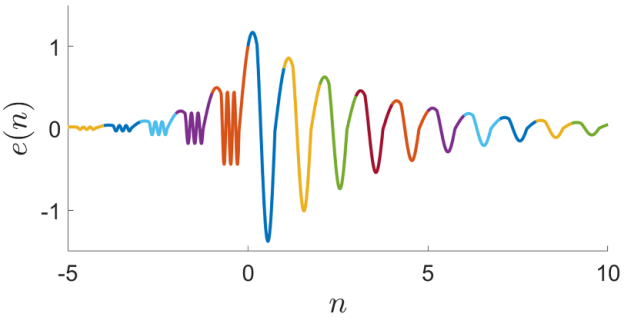

Figure 9. Same as figure 6, but the permittivity ϵ of the middle layer in the simple medium is increased 5% from 20 to 21. The normalized frequency $a/\lambda \approx 0.6808$.

and closes in the middle of the Brillouin zone. An intuitive explanation of this feature is given in the appendix.

The increase of ξ is manifest in the very narrow gap around $a/\lambda \approx 0.5$ and even more clearly in the gap $a/\lambda \sim 0.62 - 0.8$. In this wide gap, the impedance does not change from a zero to a pole or vice versa, but rather from a null to a null. This does not contradict the theory of the previous section because, in the presence of frequency dispersion of any material parameters, the mathematical problem is no longer of the Sturm–Liouville kind, and the Sturm–Liouville oscillation theory no longer applies.

This may have a dramatic impact on the b-bc principle. Indeed, let us take a closer look at the impedances around $a/\lambda \sim 0.62$ in figures 4, 10, where the respective bandgaps overlap. By our definition, the first gap is of type p, as it starts with a pole of impedance, i.e. with a symmetric mode. In the second case (anomalous dispersion), the bandgap is of type n, as it starts with a null of the impedance, i.e. an antisymmetric mode. Ordinarily, if these two structures were put together, they would form, in our terminology, a '*pn* junction,' and there would have to be a mode at an interface boundary between them. But that is not possible because both impedances are positive in the overlap range. This counterexample shows that the b-bc principle does not have to hold in the presence of arbitrary frequency dispersion. However, it does hold in the 1.5D setting for any physically

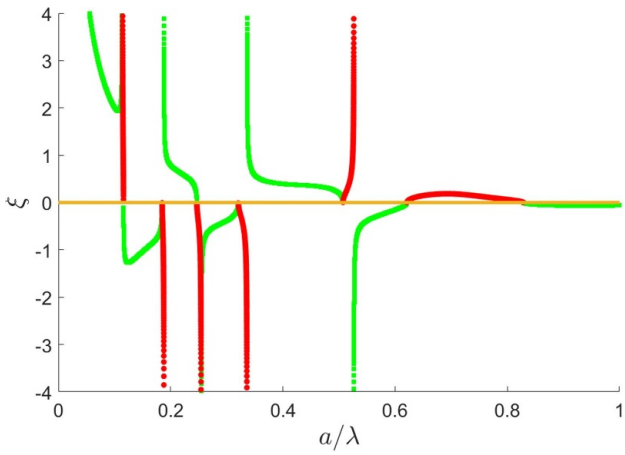

Figure 10. Same as figure 4, but for the example with anomalous dispersion; parameters are indicated in the text.

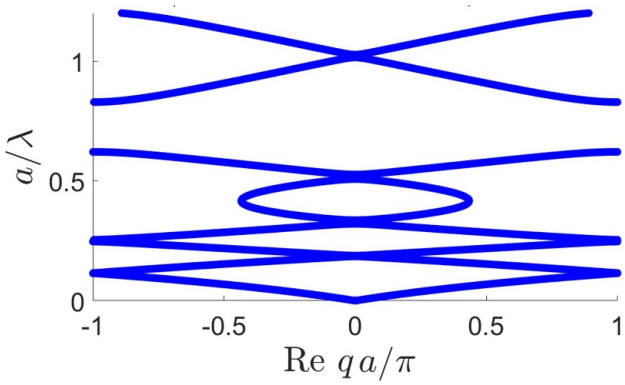

Figure 11. Bloch bands for the example with anomalous dispersion; parameters are indicated in the text.

realizable systems with a positive density of electromagnetic energy.

5. Conclusion

This paper extends the previous mathematical and physical analyses of the b-bc principle to dispersive media and waves traveling along an interface boundary between two periodic structures. This is dubbed as a '1.5D' case, since fields and wave vectors may have two nonzero Cartesian components, but the problem can be mathematically reduced to a 1D equation. The lattice cells are assumed to have mirror symmetry; losses are neglected. The main results are as follows.

The most significant finding of the paper is that the b-bc principle follows from the positivity of electromagnetic energy density. If the dispersion relation is physical—that is, if electromagnetic energy density is positive—the paper rigorously proves that in the 1.5D setup the boundary impedance within any given bandgap decreases monotonically, as it does in the non-dispersive 1D case analyzed previously [14–16]. Conversely, if this positivity is violated (in a hypothetical medium), then the b-bc principle may not hold either.

A numerical example of an interface mode has been presented. This mode survives under 5%–10% perturbations of parameters—notably, even if the mirror symmetry of the lattice cell is broken to some extent. This example should be viewed as a prototype for future case studies; the objective will be to explore possible practical uses of the interface modes. To succeed, future projects should include inverse design, optimization, fabrication, and measurements.

Data availability statement

The data that support the findings of this study are available upon reasonable request from the authors.

Appendix

To gain insight into the nonstandard behavior of some Bloch bands in the presence of frequency dispersion, it is helpful to distill the analysis to the simplest possible cases. Suppose, first, that in a homogeneous lattice cell the dielectric permittivity is a step function of frequency; as a numerical illustration, let

$$\epsilon = \begin{cases} \epsilon_1, & a/\lambda < a/\lambda_0 \\ 1, & a/\lambda \geqslant a/\lambda_0 \end{cases}, \quad \epsilon_1 = 15, \quad a/\lambda_0 = 0.3 \tag{22}$$

The respective bands, shown in figure 12, feature straight lines corresponding to the two distinct values of ϵ.

Next, let us see what happens if we smooth out the step function (figure 13; we use $\sqrt{\epsilon}$ rather than index n not to overload the symbol n in this paper):

$$\sqrt{\epsilon} = \begin{cases} \sqrt{\epsilon_1}, & a/\lambda < a/\lambda_0 \\ 1 + \left(\sqrt{\epsilon_1} - 1\right) \exp\left(-\left(a/\lambda - a/\lambda_0\right)^2 / \gamma^2\right), & \\ & a/\lambda \geqslant a/\lambda_0 \end{cases} \tag{23}$$

with $\gamma = 0.2$. Then the 'downward-pointing arrow' of figure 12 becomes curved (figure 14) and resembles figure 11.

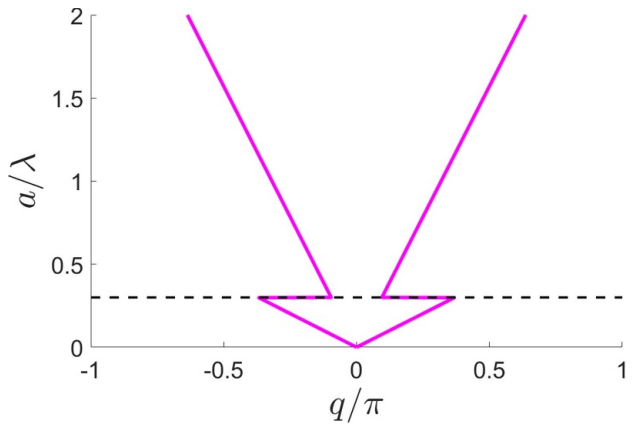

Figure 12. When ϵ is a step function (22) in a homogeneous cell, the Bloch bands feature two straight lines corresponding to the respective values of ϵ, thereby forming a 'downward-pointing arrow' pattern. The dashed line indicates the critical value $a/\lambda_0 = 0.3$.

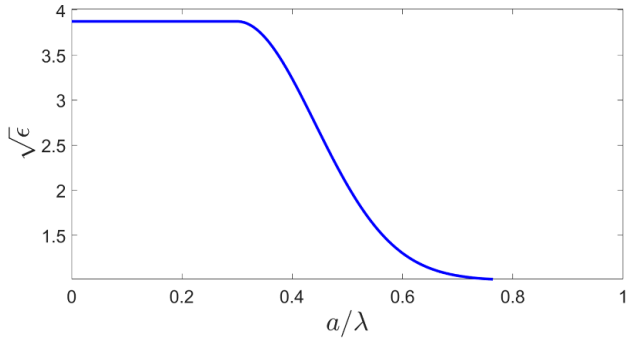

Figure 13. The smoothed out step function (23) for the dielectric permittivity.

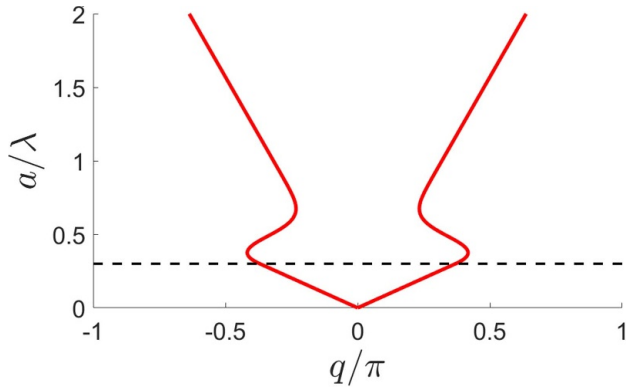

Figure 14. When ϵ is a smoothed-out step function (23) in a homogeneous cell, the 'downward-pointing arrow' pattern becomes curved. The bands near the critical value $a/\lambda_0 = 0.3$ (the dashed line) do not extend to the band edges.

ORCID iDs

Igor Tsukerman https://orcid.org/0000-0001-8318-3225
Vadim A Markel https://orcid.org/0000-0002-9748-6865

References

[1] Hasan M Z and Kane C L 2010 Colloquium: topological insulators *Rev. Mod. Phys.* **82** 3045–67
[2] Jalali Mehrabad M, Mittal S and Hafezi M 2023 Topological photonics: fundamental concepts, recent developments and future directions *Phys. Rev.* A **108** 040101
[3] Vanderbilt D 2018 *Berry Phases in Electronic Structure Theory: Electric Polarization, Orbital Magnetization and Topological Insulators* (Cambridge University Press)
[4] Prodan E and Schulz-Baldes H 2016 *Bulk and Boundary Invariants for Complex Topological Insulators* (Springer)
[5] Haldane F D M and Raghu S 2008 Possible realization of directional optical waveguides in photonic crystals with broken time-reversal symmetry *Phys. Rev. Lett.* **100** 013904
[6] Wang Z, Chong Y D, Joannopoulos J D and Soljačić M 2008 Reflection-free one-way edge modes in a gyromagnetic photonic crystal *Phys. Rev. Lett.* **100** 013905
[7] Wang Z, Chong Y, Joannopoulos J and Soljačcić M 2009 Observation of unidirectional backscattering-immune topological electromagnetic states *Nature* **461** 772–5
[8] Hatsugai Y 1993 Chern number and edge states in the integer quantum Hall effect *Phys. Rev. Lett.* **71** 3697–700
[9] Hatsugai Y 1993 Edge states in the integer quantum Hall effect and the Riemann surface of the Bloch function *Phys. Rev.* B **48** 11851–62
[10] Su W P, Schrieffer J R and Heeger A J 1979 Solitons in polyacetylene *Phys. Rev. Lett.* **42** 1698–701
[11] Thiang G C 2020 Edge-following topological states *J. Geom. Phys.* **156** 103796
[12] Mittal S, Ganeshan S, Fan J, Vaezi A and Hafezi M 2016 Measurement of topological invariants in a 2D photonic system *Nat. Photon.* **10** 180–3
[13] Xiao M, Zhang Z Q and Chan C T 2014 Surface impedance and bulk band geometric phases in one-dimensional systems *Phys. Rev.* X **4** 021017
[14] Thiang G C and Zhang H 2023 Bulk-interface correspondences for one-dimensional topological materials with inversion symmetry *Proc. R. Soc.* A **479** 20220675
[15] Tsukerman I and Markel V A 2023 Topological features of Bloch impedance *Europhys. Lett.* **144** 16002
[16] Coutant A and Lombard B 2024 Surface impedance and topologically protected interface modes in one-dimensional phononic crystals *Proc. R. Soc.* A **480** 20230533
[17] Felbacq D and Rousseau E 2024 Characterizing the topological properties of 1D non-Hermitian systems without the Berry–Zak phase *Ann. Phys., Lpz.* **536** 2300321
[18] Zak J 1989 Berry's phase for energy bands in solids *Phys. Rev. Lett.* **62** 2747–50
[19] Khanikaev A B, Mousavi S H, Tse W-K, Kargarian M, MacDonald A H and Shvets G 2013 Photonic topological insulators *Nat. Mater.* **12** 233–9
[20] Khanikaev A B and Shvets G 2017 Two-dimensional topological photonics *Nat. Photon.* **11** 763–73
[21] Banerjee A, Sarkar R, Dey S and Narayan A 2023 Non-Hermitian topological phases: principles and prospects *J. Phys.: Condens. Matter* **35** 333001
[22] Yan Q, Zhao B, Zhou R, Ma R, Lyu Q, Chu S, Hu X and Gong Q 2023 Advances and applications on non-Hermitian topological photonics *Nanophotonics* **12** 2247–71
[23] Silva S V, Fernandes D E, Morgado T A and Silveirinha M G 2022 Topological pumping and Tamm states in photonic systems *Phys. Rev.* B **105** 155133
[24] Qiu J, Lin J, Xie P and Zhang H 2023 Mathematical theory for the interface mode in a waveguide bifurcated from a Dirac point (arXiv:2304.10843)
[25] Ma T, Khanikaev A B, Hossein Mousavi S and Shvets G 2015 Guiding electromagnetic waves around sharp corners: topologically protected photonic transport in metawaveguides *Phys. Rev. Lett.* **114** 127401
[26] k^2 is denoted with s as in [14, 15], to simplify the algebraic expressions in the subsequent analysis
[27] Lin J and Zhang H 2022 Mathematical theory for topological photonic materials in one dimension *J. Phys. A: Math. Theor.* **55** 495203
[28] Shi Xi, Xue C, Jiang H and Chen H 2016 Topological description for gaps of one-dimensional symmetric all-dielectric photonic crystals *Opt. Express* **24** 18580–91
[29] Brillouin L'eon 1960 *Wave Propagation and Group Velocity* (Academic)
[30] Landau L D and Lifshitz E M 1984 *Electrodynamics of Continuous Media* (Pergamon)
[31] Tsukerman I and Markel V A 2014 A nonasymptotic homogenization theory for periodic electromagnetic structures *Proc. R. Soc.* A **470** 2014.0245
[32] Markel V A and Tsukerman I 2016 Applicability of effective medium description to photonic crystals in higher bands: theory and numerical analysis *Phys. Rev.* B **93** 224202
[33] Zayats A V, Smolyaninov I I and Maradudin A A 2005 Nano-optics of surface plasmon polaritons *Phys. Rep.* **408** 131–314
[34] Akimov Y 2018 Optical resonances in Kretschmann and Otto configurations *Opt. Lett.* **43** 1195–8
[35] Long Y, Ren J, Guo Z, Jiang H, Wang Y, Sun Y and Chen H 2020 Designing all-electric subwavelength metasources for near-field photonic routings *Phys. Rev. Lett.* **125** 157401